A fast and robust semi-analytical approach for the calculation of coil transient eddy-current response above planar specimens

Anastassios Skarlatos, Theodoros Theodoulidis, Nikolaos Poulakis

A fast and robust semi-analytical approach for the calculation of coil transient eddy-current response above planar specimens

Anastassios Skarlatos[1], *Member, IEEE*, Theodoros Theodoulidis[2], *Senior Member, IEEE*,
Nikolaos Poulakis[3], *Member, IEEE*

[1] Université Paris-Saclay, CEA, List, F-91120, Palaiseau, France
[2] Department of Mechanical Engineering, University of Western Macedonia, Kozani, 50132 Greece
[3] Department of Electrical Engineering, University of Western Macedonia, Kozani, 50132 Greece
Corresponding author: A. Skarlatos (email: anastasios.skarlatos@cea.fr).

The transient response of an induction coil above an infinite conducting plate is calculated in time domain by combining a semi-analytical modal expansion approach with the Euler integration scheme. The derived state equation at a given time-step is formally equivalent to the Helmholtz equation with an imaginary frequency linked to the sampling rate, which provides a significant computational advantage with respect to spectral methods based on Fourier/Laplace domain discretisation. In addition, time-stepping schemes prove to be more robust than the spectral approaches, where the optimal choice of the sample frequencies is an issue of major concern. The developed solution is applied for the calculation of the magnetic field in a driver-pickup coil inspection configuration involving pulsed currents, and the coil response is obtained using the time-domain version of the reciprocity theorem. The theoretical results are compared against reference numerical solutions demonstrating an excellent agreement.

I. Introduction

Pulsed eddy-current testing (PECT) has attracted the interest of numerous researchers and non-destructive testing practitioners the last years for a number of reasons. The main motivation of this increased interest is the attempt of extending the sensitivity zone of traditional harmonic ECT techniques deeper in the material. Pulsed currents, having in principle broadband spectra, can respond to this requirement, without compromising the resolution for subsurface defects thanks to the higher frequency spectral components. From the point of view of laboratory implementation, PECT can be carried out with relatively simple equipment. This convenience is also enhanced by the latest developments of fast data acquisition cards nowadays.

From the theoretical point of view, this raised interest in the PECT method has motivated the development of fast and reliable theoretical models for the prediction of the measurement signals. Semi-analytical solutions are always attractive, when the problem under consideration is amenable to analytic formulation, due to very interesting computational times with respect to numerical solutions. There is a huge amount of published works on the semi-analytical modelling of harmonic ECT in canonical multilayer structures, stemming from the seminal articles of Dodd and Deeds [1], [2]. Taking advantage of this corpus of published works, transient solutions can be constructed by addressing the eddy-current problem under a monochromatic excitation using the above mentioned established harmonic solutions and resorting to an inverse Fourier or Laplace transform to obtain the corresponding time signals. The main difference of the two approaches is the domain of the sampling frequencies, which in the case of the Laplace transform spans the half of the complex plane, whereas the Fourier frequencies lie on the imaginary axis.

The Fourier transform is perhaps the most straight forward approach for the calculation of the transient response due to the simplicity and robustness of the inverse transform operator, which in addition can take advantage of the well established Fast Fourier Transform (FFT) algorithms [3]–[5]. Even if FFT can significantly accelerate the calculation of the time signals, the increased number of frequencies required for the accurate representation of the usual transient signals met in PECT applications can inhibit the inherent excellent computational performances of the semi-analytical solutions. To overcome this problem, intelligent sampling of the frequency axis in combination with interpolation has been proposed in recent works [6]–[8]. An insurmountable difficulty inherit with the Fourier approach is the so-called Gibbs effect apparent at the vicinity of signal discontinuities, which is the case of step or pulse excitations, frequently used in PECT configurations.

Laplace transform on the other side remains the most efficient and elegant tool for the solution of initial value problems. The main challenge, however, of this approach comes from the lack of a generic and robust algorithm for the sampling of the complex plane and the thereupon linked inversion approach. As a result, the solution to the problem remains to a great extend ad hoc, with a number of works devising closed-form (whenever possible) inversion formulas [9], [10] or pole extraction using Padé approximation or decomposition using the generalised pencil of function (GPoF) approach [11], [12]. For the short-time transient signal calculation, which has the form of exponential damping, a number of specialised numerical algorithms such as the Stehfest method has also been proposed with excellent results [13].

A more direct approach, usually applied to mesh-based approaches, such as the finite element method (FEM) or the finite integration technique (FIT), relied in discretisation of the temporal derivatives and iterative solution using a time-stepping scheme [14]–[16]. Stability issues impose the use of implicit time integration schemes for diffusion problems as the one examined here. Nevertheless, recent works have shown that quasi-explicit schemes can also be applied with the consequent benefits in computational performances [16].

This latter approach has been barely considered, to the best of he authors' knowledge, in combination with modal schemes, and the reason lies with the right-hand term in the diffusion equation linked with the previous timestep(s). Such inhomogeneous terms may be resolved with the extension of the modal projection basis, as it was shown in the case of non-linear eddy-current problem [12], [17].

In this work, the ideas developed in [12], [17] are applied for the solution of the implicit time-stepping schemes obtained from the temporal discretisation of the eddy-current equation of state in the spectral domain for the solution of the PECT inspection of a conducting plate. The interest in combining the spectral (semi-analytical) approach with time-stepping relies in the robustness of the approach regardless the form of the excitation signal. It is shown that the state equation obtained upon time-discretisation bears the same form with the harmonic case with an effective frequency (linked with the discretisation rate), which is the same for all time-steps (provided that a uniform discretisation has been applied). This detail is important for the efficiency of the overall scheme since combined with the sparsity of the system matrix obtained upon the projection to the spectral basis (the problem modes) is translated to a problem factorisation. A time-domain version of the reciprocity theorem is then proposed in order to calculate the induced electromotive force (EMF) at the pick-up coil without the need of passing from the Fourier domain.

The paper is organised as follows. The considered problem is presented in section II. The mathematical formulation of the approach is developed in the next section (section III), followed by the calculation of receiving coil EMF in section IV. An analysis of the numerical performance of the method is presented in section V. Finally, the numerical results obtained by the proposed approach are compared against reference solutions in section VI.

II. PROBLEM DESCRIPTION

The problem which we shall consider is depicted in Fig. 1. An infinite conducting plate of thickness d is inspected by a couple of cylindrical coaxial coils, whose axes are perpendicular to the surface of the plate. The plate conductivity and magnetic permeability is equal to σ and $\mu = \mu_r \mu_0$, respectively, with μ_0 standing for the permeability of the free space and μ_r is the relative permeability. The coils are connected in driver-pickup mode, that is, current is supplied to the first one (driver coil), and the induced voltage at the second (pickup coil) is measured.

The excitation current has arbitrary temporal profile $I = I(t)$, whose energy is principally distributed in the low-frequency band between 0 and 100 kHz. Under this assumption, the quasi-static approximation for the Maxwell equations is valid, and we can proceed to the analysis in a similar way that we do for the typical harmonic eddy-current problem. In addition, the coil current is assumed to be weak enough in order that non-linear effects be negligible.

For the needs of the analysis, the three layers of the geometry (plate and air columns above and underneath it) will be referred to using the indices 1, 2 and 3, as shown in Fig. 1.
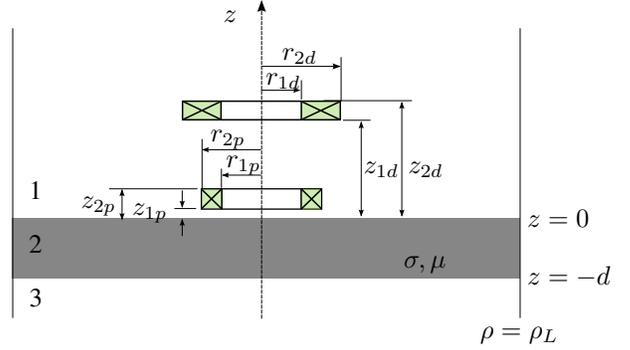

Fig. 1: Infinite conducting plate inspected via a pair of coaxial cylindrical coils connected in driver(d) - pickup (p) mode. The geometry consists a three-layer medium.

The objective of the analysis is to calculate the induced voltage in the coil $V(t)$.

It is convenient to artificially truncate the computational domain at a sufficiently remote from the coil distance, which will be denoted as $\rho_r L$ and apply a perfectly electric conductor (PEC) condition there. Since we are dealing with a diffusion problem, the field intensity is rapidly decreasing as we are moving far from the source, and hence it can be considered as negligible after a certain distance. This is the basic assumption adopted in the so called truncated region eigenfunction (TREE) approach, used in this work and which proves to result in a convenient simplification of the problem (with respect to the classical Dood and Deeds approach [1], [2]).

III. SOLUTION IN THE TIME DOMAIN USING TIME DESCRETISATION

A. Vector potential formulation in time domain

The mathematical analysis of the transient problem follows the $\mathbf{A} - \Phi$ formulation for the quasi-static limit, which is the established approach for the treatment of axisymmetric problems. The magnetic vector potential $\mathbf{A}$, and the electric scalar potential Φ are defined via the relations

$$\mathbf{B} = \nabla \times \mathbf{A} \qquad (1)$$

and

$$\mathbf{E} = -\frac{d\mathbf{A}}{dt} - \nabla \Phi \qquad (2)$$

with $\mathbf{E}$, $\mathbf{B}$ being the electric field and the magnetic flux density, respectively. Notice that for problems with axisymmetric summetruy we can adopt a potential ansatz of the type $\mathbf{A} = A\mathbf{e}_\phi$, where $\mathbf{e}_\phi$ is the unit vector along the ϕ direction, i.e. the magnetic vector potential lies in the azimuthal direction.

Upon substitution to the Maxwell equations one obtains the diffusion equation for the potentials

$$\nabla \times \mu^{-1} \nabla \times \mathbf{A} + \sigma \frac{d\mathbf{A}}{dt} = -\sigma \Phi + \mathbf{J} \qquad (3)$$

where $\mathbf{J}$ is the excitation current density, and σ, μ stand for the electrical conductivity and the magnetic permeability of the medium. The material will be considered as isotropic and linear throughout this work, i.e. the magnetic flux density $\mathbf{B}$

and the magnetic field **H** are related via a linear constitutive relation

$$\mathbf{B} = \mu\mathbf{H}. \tag{4}$$

Assuming in addition a piecewise homogeneous material and using the Coulomb's gauge for the magnetic vector potential **A**, the magnetic permeability can be drawn outside the curl operator reducing (3) to the scalar equation

$$\left(\nabla^2 - \frac{1}{\rho^2} - \mu\sigma\frac{d}{dt}\right) A = -\mu J, \tag{5}$$

where we have taken into account the azimuthal orientation of the magnetic potential and the excitation current ($\mathbf{J} = J\mathbf{e}_\phi$).

We are interested in the source-free case $J = 0$, since all the layers except the internal and/or the external region of the tube wall do not contain excitation currents. The coil field in these latter two regions will be treated indirectly as we will see later.

Equation (5) is a parabolic equation, and hence its numerical integration should be carried out using an unconditionally stable scheme. Let us consider a homogeneous discretisation of the time axis $t_i = i\Delta t$, with $i = 0, 1, \ldots$ and Δt the discretisation step. Using an implicit Euler scheme for the time derivative, (5) reduces to the following update equation, where the solution at i is given by means of the solution at the previous time-step $i - 1$

$$\left(\nabla^2 - \frac{1}{\rho^2} - \frac{\mu\sigma}{\Delta t}\right) A_i = -\frac{\mu\sigma}{\Delta t} A_{i-1}. \tag{6}$$

The notation can be simplified by introducing the equivalent angular frequency $\omega_s = -\sqrt{-1}/\Delta t$, with $\sqrt{-1}$ being the imaginary unit, and (6) becomes

$$\left(\nabla^2 - \frac{1}{\rho^2} - k^2\right) A_n = -f_n. \tag{7}$$

with $k^2 = \sqrt{-1}\omega_s\mu\sigma$ and $f_n = k^2 A_{n-1}$. Equation (7) is formally equivalent with the inhomogeneous Helmholtz equation for frequency equal to the discretisation (sampling) frequency of the time integration scheme. Our problem thus reduces to the solution of the Helmholtz equation with a source term at each time-step, which is a very convenient observation since one can resort to tools developed for the harmonic regime in a planar medium [12], [17]–[19].

B. General solution of the inhomogeneous Helmholtz equation

For the solution of (7), we shall adopt the same strategy used in [12], [17]. The solution of the inhomogeneous equation is decomposed in the sum of a partial solution, which eliminates the right-hand-side term, and the solution of the homogeneous equation, which takes care of the current excitation and assures the fulfilment of the continuity relations across the geometry interfaces.

In the two air regions, above and underneath the plate both k and f_i in the diffusion equation (6) vanish, which means that

the problem there reduces to the magnetostatic formulation[1]. The solution for the magnetic potential in these two regions reads

$$A_i^{(1)}(\rho, z) = \sum_{m=1}^{\infty} J_1(\kappa_m\rho)\left[C_{i;m}^{(1)}e^{\kappa_m z} + D_{i;m}^{(s)}e^{-\kappa_m z}\right] \tag{8}$$

and

$$A_i^{(3)}(\rho, z) = \sum_{m=1}^{\infty} C_{i;m}^{(3)} J_1(\kappa_m\rho)\, e^{-\kappa_m z} \tag{9}$$

respectively. Note that $D_{im}^{(s)}$ stand for the development coefficients for the coil field in the unbounded medium, and they are hence known. Their explicit expressions will be given at a later point. The κ_m eigenvalues are determined by the zero tangential potential condition imposed by the PEC boundary at ρ_L, and they are obtained by the roots of the Bessel functions

$$J_1(\kappa_m\rho_L) = 0, \quad m = 1, 2, \ldots, \infty. \tag{10}$$

Inside the plate, we must address the inhomogeneous Helmholtz equation. The general solution can be expressed as the superposition of the homogeneous solution and a special solution, which satisfies the right-hand-side [17], [20]

$$A_i^{(2)}(\rho, z) = A_i^{(h)}(\rho, z) + A_i^{(s)}(\rho, z) \tag{11}$$

The homogeneous solution reads

$$A_i^{(h)}(\rho, z) = \sum_{m=1}^{\infty} J_1(\kappa_m\rho)\left[C_{i;m}^{(2)}e^{v_m z} + D_{i;m}^{(2)}e^{-v_m z}\right] \tag{12}$$

with $v_m^2 = \kappa_m^2 + k^2$.

The modal basis used for the homogeneous solution belongs to the kernel of the Helmholtz operator ($\ker\left[\nabla^2 - k^2\right]$) and hence must be complemented in the z direction for the development of the special solution, which must satisfy a non-zero right-hand side [15], [17]. A suitable eigenbasis for this development is the Fourier basis. Since the solution does not satisfy any symmetry property along z the full Fourier basis must be used with period slightly larger than d (given that a Fourier series describes a periodic function). Such choice, however, would suffer from the Gibbs effect at the plate boundaries. To overcome this difficulty, the special solution can be split into two terms: one satisfying zero boundary conditions at the plate interfaces, and a second term accounting for the in general non-zero field value at those interfaces. This representation is schematically shown in Fig. 2. We can thus write

$$A_i^{(s)}(\rho, z) = \sum_{m=1}^{\infty} J_1(\kappa_m\rho) \sum_{n=1}^{\infty} \left[c_{i;mn}\sin(q_n z) + g_{i;m}(z)\right] \tag{13}$$

with eigenvalues q_n being obtained by the zero field condition at the plate interfaces, namely

$$q_n = \frac{n\pi}{d}, \quad n = 1, 2, \ldots, \infty. \tag{14}$$

[1]Strictly speaking, the field is not stationary but its value follows the excitation variations instantaneously, that is without delay due to diffusion. In this sense the problem formulation is isomorphic with the magnetostatic equations and hence it will be considered as such.

We are free to chose the form of the $g_{i;m}(z)$ with the condition that it contains a sufficient number of degrees of freedom in order to account for the field values at $z = 0$ and $z = -d$. These conditions are easily met by any polynomial of degree greater than 0. Another possible choice is

$$g_{i;m}(z) = \sum_{n=1}^{2} d_{i;mn} \cos(q_n z) \tag{15}$$

with q_n given by (14) and the coefficients $d_{i;mn}$ are determined by matching the boundary values for $g_{i;m}(z)$. In this work, this latter choice has been adopted since it leads to slightly simpler equations.
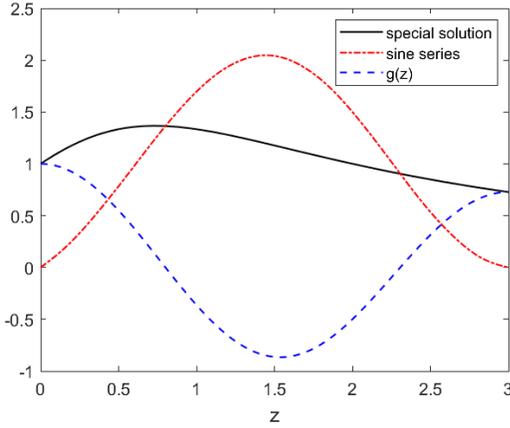

Fig. 2: Representation of an arbitrary function as a sum of a sine series and a residual term.

C. Application of the update equation: special solution calculation

Substituting (11) into (6), the first two terms vanish by construction (being solutions of the homogeneous equation) yielding

$$\sum_{m=1}^{\infty} J_1(\kappa_m \rho) \left[\sum_{n=1}^{\infty} \left(v_m^2 + q_n^2 \right) c_{i;mn} \sin(q_n z) \right.$$
$$\left. + \sum_{n=1}^{2} \left(v_m^2 + q_n^2 \right) d_{i;mn} \cos(q_n z) \right] = f_i(\rho, z). \tag{16}$$

The $d_{i;mn}$ coefficients are easily obtained by observing (16) at the two plate interfaces (thus the first term vanishes) and weighting the two sides of the equation by the radial eigenfunctions $J_1(\kappa_m \rho)$

$$d_{i;mn} = \frac{\langle J_1(\kappa_m \rho), f_i(\rho, 0) \mp f_i(\rho, -d) \rangle}{2 \left(v_m^2 + q_n^2 \right)}, \quad n = 1, 2 \tag{17}$$

with the minus sign being chosen for $n = 1$ and the plus for $n = 2$. The inner product is defined as

$$\langle J_1(\kappa_m \rho), R(\rho) \rangle := \frac{2}{\rho_L^2 J_0^2(\kappa_m \rho_L^2)} \int_0^{\rho_L} \rho J_1(\kappa_m \rho) R(\rho) \, d\rho. \tag{18}$$

Recalling the definition of f_i, which stands for the previous timestep solution, i.e. $f_i = k^2 A_{i-1}^{(2)}$ and substituting the corresponding modal development, (17) reduces to

$$d_{i;mn} = \frac{k^2}{v_m^2 + q_n^2} \left[d_{i-1;mn} + \frac{1}{2} \left(1 \mp e^{-v_m d} \right) C_{i-1;m}^{(2)} \right.$$
$$\left. + \frac{1}{2} \left(1 \mp e^{v_m d} \right) D_{i-1;m}^{(2)} \right], \quad n = 1, 2. \tag{19}$$

Note that $C_{i-1;m}, D_{i-1;m}^{(2)}$ and $d_{i-1;mn}$ are known since they have been calculated in the previous step.

Having evaluated $a_{i;m}$ and $b_{i;m}$, we can move this term to the right-hand-side of (16) and weight both terms with the Laplacian operator eigenfunctions $J_1(\kappa_m \rho) \sin(q_n z)$ thus obtaining

$$c_{i,mn} = \frac{1}{v_m^2 + q_n^2} \langle J_1(\kappa_m \rho) \sin(q_n z), f_i(\rho, z) \rangle, \quad n = 1, \dots, \infty \tag{20}$$

with the inner product along ρ being given by (18) and the inner product along z defined as

$$\langle \sin(q_n z), Z(z) \rangle := \frac{2}{d} \int_{-d}^{0} \sin(q_n z) Z(z) \, dz. \tag{21}$$

Recalling again the f_i definition as the solution at the previous timestep, (22) becomes

$$c_{i,mn} = \frac{k^2}{v_m^2 + q_n^2} \left[c_{i-1;mn} + C_{i-1;m}^{(2)} M_{mn} + D_{i-1;m}^{(2)} N_{mn} \right],$$
$$n = 1, \dots, \infty \tag{22}$$

with the integrals

$$\left\{ \begin{array}{c} M_{mn} \\ N_{mn} \end{array} \right\} = \frac{2}{d} \int_{-d}^{0} \sin(q_n z) \, e^{\pm v_m z} dz$$
$$= -\frac{2}{d} \frac{q_n}{v_m^2 + q_n^2} \left[1 - e^{\mp v_m d} (-1)^n \right]. \tag{23}$$

D. Application of the continuity relations: homogeneous solution calculation

The development coefficients of the homogeneous solution $C_{i;m}^{(1)}, C_{i;m}^{(2)}, D_{i;m}^{(2)}$ and $D_{i;m}^{(3)}$ will be determined by the application of the continuity relations at the interfaces of the geometry. We have two conditions in our procession which the solution must satisfy: the continuity of the magnetic potential and its normal derivative. Hence at the $z = 0$ interface we have

$$A^{(1)} \Big|_{\rho_1} = A^{(2)} \Big|_{\rho_1} \tag{24}$$

$$\frac{\partial A^{(1)}}{\partial z} \Big|_{\rho_1} = \frac{1}{\mu_r} \frac{\partial A^{(2)}}{\partial z} \Big|_{\rho_1} \tag{25}$$

and similarly for $z = -d$.

Substituting the expressions (8)-(11) and weighting with the radial eigenfuction using (18), we obtain for z_0

$$C_{i;m}^{(1)} + D_{i;m}^{(s)} = C_{i;m}^{(2)} + D_{i;m}^{(2)} + \sum_{n=1}^{2} d_{i;m1} \qquad (26)$$

$$\mu_r \kappa_m \left[C_{i;m}^{(1)} - D_{i;m}^{(s)} \right] = v_m \left[C_{i;m}^{(2)} - D_{i;m}^{(2)} \right] + \sum_{n=1}^{\infty} q_n c_{i;mn}. \qquad (27)$$

In the same fashion the continuity relations at $z = -d$ yield

$$C_{i;m}^{(3)} = C_{i;m}^{(2)} + D_{i;m}^{(2)} + \sum_{n=1}^{2} (-1)^n d_{i;mn}. \qquad (28)$$

$$\mu_r \kappa_m C_{i;m}^{(3)} = v_m \left[C_{i;m}^{(2)} - D_{i;m}^{(2)} \right] + \sum_{n=1}^{\infty} (-1)^n q_n c_{i;mn}. \qquad (29)$$

E. Source field

In the previous development, the field of the source coil in the air, represented in the modal solution via the coefficients $D_{i;m}^{(s)}$ has been considered as known. In order to calculate these coefficients, one has to recall that the coil field will satisfy the magnetostatic equations, since $\sigma = 0$ in air, and hence (5) reduces to

$$\left(\nabla^2 - \frac{1}{\rho^2} \right) A_0(\rho, z, t) = -\mu J(\rho, z, t) . \qquad (30)$$

It becomes clear from (30) that the solution A_0 follows instantaneously the current density value, which in its turn can be split in a spatial and a temporal part.

$$J(\rho, z, t) = \iota(\rho, z) I(t) \qquad (31)$$

with

$$\iota(\rho, z) = \begin{cases} \frac{N_d}{(r_{2d} - r_{1d})(z_{2d} - z_{1d})}, & \text{in coil.} \\ 0 & \text{elsewhere} \end{cases} \qquad (32)$$

N_d stands for the number of turns in the driving coil, and $r_{1d}, r_{2d}, z_{1d}, z_{2d}$ its radial and axial dimensions, shown in Fig. 1.

Following [18], $D_{i;m}^{(s)}$ are given from the relation

$$D_{i;m}^{(s)} = -4\mu_0 \iota(\rho, z) \sinh\left(\frac{\kappa_m l}{2} \right) \frac{\chi(\kappa_m r_{1d}, \kappa_m r_{2d})}{\kappa_n^5 \left[\rho_L J_1(\kappa_n \rho_L) \right]^2}$$

$$\times J_m(\kappa_n \rho_d) e^{-\kappa_m z_d} I_i \qquad (33)$$

where $r_d = (r_{2d} + r_{1d})/2$ and $z_d = (z_{2d} + z_{1d})/2$ the coordinates of the coil centre and $l = z_{2d} - z_{1d}$ its length. I_i stands for the discretised current signal, i.e. $I_i = I(t_i)$.

IV. CALCULATION OF THE PICK-UP COIL VOLTAGE

For the driver-pick-up coil configuration that we examine here, an important quantity is the electromotive force (EMF) induced at the pick-up coil, for the reason that it constitutes the main experimental variable for this type of control. Its calculation is thus one of the major objectives of the mathematical modelling.

In harmonic regime, the respective quantity (or the equivalent variable of the coil mutual impedance) is calculated in

an elegant way using the Auld's reciprocity theorem [21], [22]. For transient measurements, this theorem can be readily extended using convolution integrals. The TD case has been treated principally in the antennas community for the calculation of receiver response to arbitrary signals [23]–[29]. To the best of the authors' knowledge, this problem has been scarcely explored for low-frequency problems and therefore it will be considered herein in some detail.

The general form for the 2D problem with rotational symmetry reads

$$\Delta V(t) * I(t) = \frac{1}{\mu_0} \oint_{\partial V} \left(A_{ec} * \nabla \frac{dA_s}{dt} - \frac{dA_s}{dt} * \nabla A_{ec} \right) \cdot d\mathbf{S} \qquad (34)$$

It is obtained following the standard procedure found in almost all the classical textbooks. A detailed derivation is provided in the appendix for the sake of the text self-completeness.

Interestingly, the convolution integral of (34) right-hand-side can be dropped by observing that the source field, being solution of the magnetostatic problem, instantly follows the time variations of the input current. Note that this is an approximation which holds only in the context of the low-frequency quasi-static formulation, which the eddy-current problem satisfies. By virtue of this property, the time derivatives of the source field will provide Dirac functions in case that the current excitation is a Heaviside function $H(t)$. Equation (34) becomes

$$\Delta s(t) = \frac{1}{\mu_0} \oint_{\partial V} \left[A_{ec}(t) \nabla A_s^* - A_s^* \nabla A_{ec}(t) \right] \cdot d\mathbf{S} \qquad (35)$$

where A_s^* is the source field for a unit constant current and Δs is the EMF integral

$$s(t) = \int_0^t \Delta V(\tau) \, d\tau. \qquad (36)$$

The EMF expression for an arbitrary current profile $I(t)$ can be easily obtained from the step response $\Delta s(t)$ by applying the Duhamel's integral [11]

$$\Delta V_I(t) = \frac{d}{dt} \int_0^t \Delta V_H(\tau) I(t - \tau) \, d\tau \qquad (37)$$

with the ΔV_I and ΔV_H denoting the signals for the arbitrary and step excitation, respectively. Noting that ΔV_H is the time derivative of $s(t)$ and carrying out integration by parts (37) becomes

$$\Delta V_I(t) = -\frac{d}{dt} \int_0^t s(\tau) \dot{I}(t - \tau) \, d\tau. \qquad (38)$$

For a discrete signal, the time integral reduces to a simple trapezoidal rule. Furthermore, the derivative can be approxi-

mated by a finite difference scheme yielding to the following relation

$$\Delta V_{Ii} = -\sum_{k=0}^{i} s_k \dot{I}_{i-k} + \sum_{k=0}^{i-1} s_k \dot{I}_{i-k-1}$$
$$= \sum_{k=0}^{i-1} s_k \left(\dot{I}_{i-k-1} - \dot{I}_{i-k} \right) - s_i \dot{I}_0. \quad (39)$$

A case of special interest consists the excitation with a rectangular pulse since this is the most usual excitation signal used in PECT applications. In this case the EMF calculation can be readily derived noting that

$$\Delta V_I(t) = \frac{d}{dt} \left[s(t) - s(t-T) \right] \quad (40)$$

where T stands for the pulse duration. Assuming that $T = K\Delta t$, the discrete form of (40) admits the particularly simple expression

$$\Delta V_{Ii} = (s_i - s_{i-1} - s_{i-K} + s_{i-K-1}) / \Delta t. \quad (41)$$

We need now to calculate the surface integral in terms of the development coefficients $C_{i;m}^{(1)}$ and $D_{i;m}^{(s)}$. The analysis is strictly identical with the harmonic case, and the result reads for the ith timestep

$$s_i = -\frac{2\pi \rho_L^2}{\mu_0} \sum_{m=0}^{\infty} \kappa_m J_1(\kappa_m \rho_L) C_{i;m}^{(1)} D_m^{(s)}. \quad (42)$$

where the timestep index i has been intentionally suppressed since the source field is constant for $t > 0$.

The absolute signal at the pickup coil can be easily obtained by recalling that for two coils in air

$$V_0(t) = -M \frac{dI}{dt} \quad (43)$$

where M is the mutual impedance between driver and pickup coil. The total signal will be the superposition of ΔV and the signal in air, i.e. $V(t) = \Delta V(t) - M\dot{I}(t)$.

V. Numerical Performance

A number of tuning parameters needs to be fixed in order to proceed to numerical computations. Rules of thump for the estimation of the domain truncation limit ρ_L and the maximum number of radial modes N_m taken into account for the solution have been proposed in a series of previous works (e.g. [18], [30], [31]). The choice of ρ_L is principally dictated by geometrical criteria such as the coil external radii. For the series truncation, general rules are more hard to find yet numerical experimentation proves that a number between 100 and 150 modes would be sufficient for the most of the cases.

As far as the number of axial modes q_l is concerned, there is again no general rule than can be followed. However, the small thickness of the specimens considered in PECT applications indicate that truncating the Fourier series to no more than 15-20 terms, would hardly affect the accuracy of the solution. The arguments resemble the discussion given in [12], [31] concerning the series truncation for the TM potential (W_b second order vector potential) in planar specimens with a

borehole. Final judge for a safe estimation of these parameters should be the numerical experimentation.

An important speed-up of the time-stepping approach with respect to spectral decomposition using Fourier or Laplace transform, consists in the fact that the sampling frequency appearing in the Helmholtz equation (7) is the same for all iterations, meaning that the system can be factorised using LU decomposition once thus significantly accelerating the overall solution. It is noted that the equation system (27),(29) is diagonal along the ϕ direction, a fact that facilitates the factorisation. A similar decomposition has been exploited also in a hybrid FIT-modal scheme leading to important speed-up factors [32]. As a figure of merit, all the numerical computations carried out in the context of this work were of the order of a few seconds for a complete excitation cycle of 100 timesteps, using a modern PC (Intel(R) Core(TM) i7-8850H CPU @ 2.60 GHz).

VI. Results

The proposed approach has been applied for the calculation of the PECT response in the inspection scenario described by Fig. 1. The plate conductivity and relative magnetic permeability are $\sigma = 5$ MS/m and $\mu_r = 150$, respectively, which correspond more or less the parameters of a typical construction steel. The plate thickness is 1 mm. The inner and outer radius of the driver coil is $r_{1d} = 1$ mm and $r_{2d} = 2.65$ mm, respectively, its length is $z_{2d} - z_{1d} = 2$ mm and its number of turns is $N_d 336$. The corresponding dimensions for the pickup coil are $r_{1p} = 2$ mm and $r_{2d} = 5$ mm and $z_{2p} - z_{1p} = 2$ mm, and it is wound with N_p=700 turns.

The first computation concerns the magnetic field calculation at a representative point in underneath the plate ($\rho_o = 0$ mm, $z_o = -3d/2$). Two waveforms for the input current have been considered: a rectangular pulse and a pulse with exponential relaxation. The latter case is representative of a realistic current signal provided by a square voltage generator. The pulse duration is taken of 1 ms duration with a 40% duty cycle (dc) for both waveforms, and the pulse amplitude reaches 1 A. The time constant for the exponential pulse is 0.05 ms. The signal waveform is depicted in Fig. 3

The field transients for both inputs are shown in Fig. 4. As reference solution are taken numerical simulations using the FIT method. The FIT solution is also calculated in TD using a timestepping scheme and the difference with the herein presented approach consists in the discretisation of the spatial part using a computational grid [14], [15].

The induced EMF signals computed with the semi-analytical approach for the two signals of Fig. 3 are compared against the corresponding FIT results in Fig. 5. Since the rectangular pulse is a highly idealised situation, the exponential curve described by the second signal is taken as a characteristic current profile when the coil is fed by a typical voltage source [9]. Note that the EMF response is calculated with FIT via direct integration of the magnetic vector potential

$$V = -2\pi \frac{N_p}{S_p} \frac{d}{dt} \int_{pickup} A(\mathbf{r}) \, dS \quad (44)$$
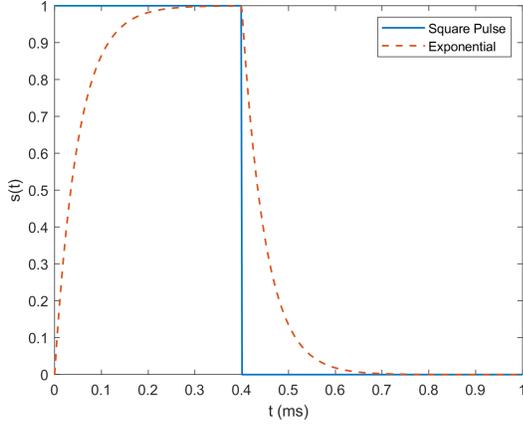
Fig. 3: Excitation signals used for the solution validation: 40% dc square pulse and pulse with exponential relaxation (charge-discharge mode).

(a)

(b)

Fig. 4: Semi-analytical vs. numerical (FIT) solution for (a) B_ρ and (b) B_z field components as a function of time at the selected observation point under the specimen. The transient signals are shown for both current excitations of Fig. 3.

where the integration is carried out on the cross-section of the pickup coil, with $S_p = (z_{2p} - z_{1p})(r_{2p} - r_{1p})$ and N_p/S_p standing for the windings density.

A final comparison is realised between the semi-analytical results for the EMF in the pickup coil calculated using the timestepping approach and the TD reciprocity theorem and the corresponding results obtained using the Laplace approach described in [13], where the Stehfest algorithm is used for the calculation of the inverse Laplace transform. The calculations have been carried out for step excitation since the Stehfest algorithm does not work for non-monotonous excitations. The comparison is shown in Fig. 6

All results show a very good agreement verifying the accuracy of the TD approach.

VII. CONCLUSION

In this work the TREE semi-analytical approach has been combined with time-stepping integration for the calculation of the eddy-current transient response under arbitrary signals. The main advantage of the time-stepping approach with respect to Fourier or Laplace inversion is the robustness of the solution (Gibbs effect or instabilities due to non-monotonicity of the input). To the drawbacks of the approach can be counted the mathematicam complexity of the scheme (one has to deal with the inhomogeneous Helmholtz equation) and the potentially large number of time samples one has to consider for certain excitations. Laplace-based approaches are much more flexible, providing the possibility of a highly inhomogeneous sampling of the time-axis. Hence, the herein presented approach can be considered as complementary to the Laplace solutions for situations where smooth transients in a reasonable time interval need to be calculated.

The TD version of the reciprocity theorem provides an elegant way of calculation the receiver EMF. Note that the approach presented in section IV is compatible with Laplace calculations of the step response, making the algorithm also applicable beyond the scope of the time-stepping solution of this work.
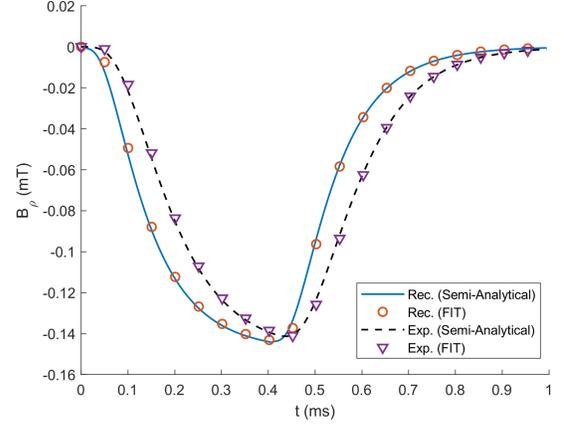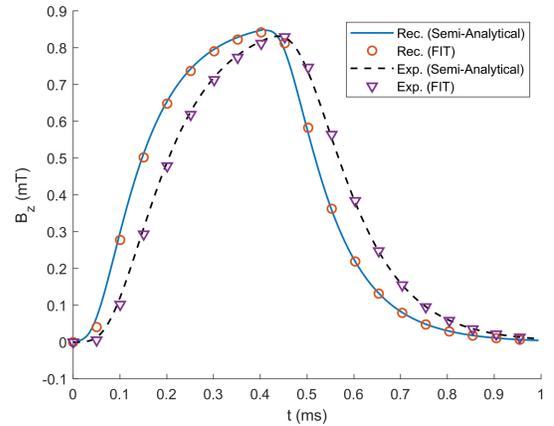
APPENDIX

In this appendix, we shall derive the TD version of the reciprocity theorem for the special case of the eddy-current problem. The derivation will follow in general Felsen and Marcuvitz [33]. Further references can be sought mostly in the wave propagation literature such as [23]–[29]. The list does not claim exhaustiveness.

We start the analysis by writing the Maxwell equations in the free space for an arbitrary current source vector $\mathbf{J}$

$$\nabla \times \mathbf{E}_s = -\frac{d\mathbf{B}_s}{dt} \tag{45}$$

$$\nabla \times \mathbf{H}_s = \mathbf{J} \tag{46}$$

where the index s stands for *source*. Introducing the conductive medium, and subtracting the free-space solution from the one in the presence of the conductor, we obtain for the field difference in the source region (the air region where source

the untransformed equation $\mathbf{E}$ and $\mathbf{H}$, via the relations

$$\mathbf{E}_{ec}^\dagger(\mathbf{r},t) = \mathbf{E}_{ec}(\mathbf{r},t'-t) \tag{51}$$

$$\mathbf{H}_{ec}^\dagger(\mathbf{r},t) = \mathbf{H}_{ec}(\mathbf{r},t'-t). \tag{52}$$

The magnetic induction $\mathbf{B}^\dagger$ is defined accordingly.

Following the usual procedure, we multiply (45),(46) with $\mathbf{H}_{ec}^\dagger$ and $\mathbf{E}_{ec}^\dagger$ and (47),(48) with $\mathbf{H}_s$ and $\mathbf{E}_s$, respectively, use of the vector identity

$$\nabla \cdot (\mathbf{A} \times \mathbf{B}) = \mathbf{B} \cdot \nabla \times \mathbf{A} - \mathbf{A} \cdot \nabla \times \mathbf{B}$$

one gets after some trivial manipulations

$$\nabla \cdot \left(\mathbf{E}_{ec}^\dagger \times \mathbf{H}_s - \mathbf{E}_s \times \mathbf{H}_{ec}^\dagger \right)$$
$$= -\mathbf{H}_{ec}^\dagger \cdot \frac{d\mathbf{B}_s}{dt} - \mathbf{H}_s \cdot \frac{d\mathbf{B}_{ec}^\dagger}{dt} - \mathbf{E}_{ec}^\dagger \cdot \mathbf{J} \tag{53}$$

and multiplying with the permeability of the free-space μ_0

$$\nabla \cdot \left(\mathbf{E}_{ec}^\dagger \times \mathbf{B}_s - \mathbf{E}_s \times \mathbf{B}_{ec}^\dagger \right) = -\frac{d}{dt} \left(\mathbf{B}_{ec}^\dagger \cdot \mathbf{B}_s \right) - \mu_0 \mathbf{E}_{ec}^\dagger \cdot \mathbf{J}. \tag{54}$$

Integrating (54) throughout the air region and applying the Gauss theorem in order to get rid of the divergence operator, we obtain

$$-\oint_{\partial V} \left(\mathbf{E}_{ec}^\dagger \times \mathbf{B}_s - \mathbf{E}_s \times \mathbf{B}_{ec}^\dagger \right) \cdot d\mathbf{S}$$
$$= \frac{d}{dt} \int_V \mathbf{B}_{ec}^\dagger \cdot \mathbf{B}_s dV + \mu_0 \int_V \mathbf{E}_{ec}^\dagger \cdot \mathbf{J} dV \tag{55}$$

where $d\mathbf{S}$ stands for the outwards pointing normal to the boundary ∂V vector.

Using (1),(2), the integrand of the boundary integral can be written successively

$$\mathbf{E}_{ec} \times \mathbf{B}_s - \mathbf{E}_s \times \mathbf{B}_{ec}$$
$$= \frac{d\mathbf{A}_{ec}}{dt} \times (\nabla \times \mathbf{A}_s) + \frac{d\mathbf{A}_s}{dt} \times (\nabla \times \mathbf{A}_{ec})$$
$$= \frac{d}{dt} (\mathbf{A}_{ec} \times \nabla \times \mathbf{A}_s) - \mathbf{A}_{ec} \times \left(\nabla \times \frac{d\mathbf{A}_s}{dt} \right)$$
$$+ \frac{d\mathbf{A}_s}{dt} \times (\nabla \times \mathbf{A}_{ec})$$

and recalling that in the 2D problem the magnetic potential is lying along the azimuthal direction $\mathbf{A} = A\mathbf{e}_\phi$, the last relation reduces to

$$\mathbf{B}_s \times \mathbf{E}_{ec} - \mathbf{E}_s \times \mathbf{B}_{ec} = \frac{d}{dt} (\mathbf{A}_{ec} \times \nabla \times \mathbf{A}_s)$$
$$- \left(A_{ec} \nabla \frac{dA_s}{dt} - \frac{dA_s}{dt} \nabla A_{ec} \right).$$
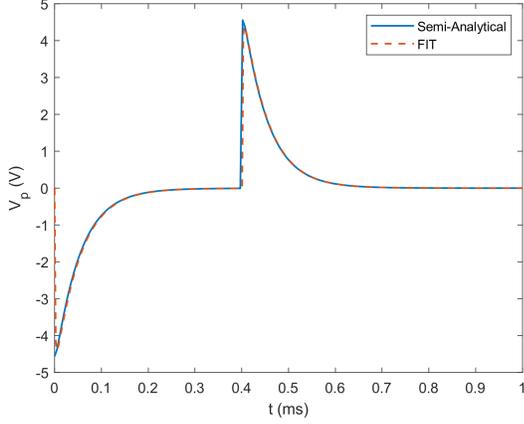

Fig. 5: EMF at the pick-up coil for the exponential pulse. The semi-analytical results calculated via the TD reciprocity relation are compared against the FIT results calculated by direct integration of the induced voltage (44).
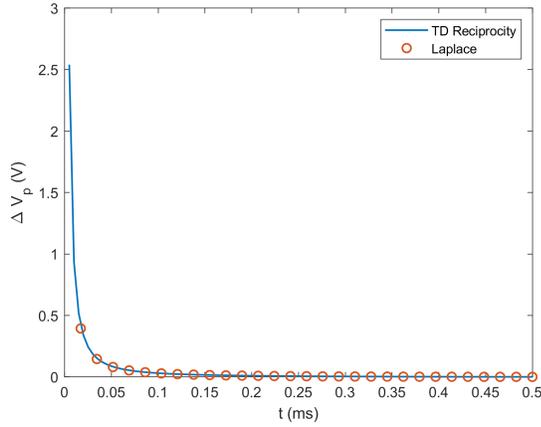

Fig. 6: Comparison of the semi-analytical calculation of the pickup EMF using the TD and the Laplace domain approach (Stehfest) for a step excitation.

lies in)

$$\nabla \times \mathbf{E}_{ec} = -\frac{d\mathbf{B}_{ec}}{dt} \tag{47}$$

$$\nabla \times \mathbf{H}_{ec} = \mathbf{0} \tag{48}$$

with $\mathbf{E}_{ec} = \mathbf{E} - \mathbf{E}_s$ and similarly for the magnetic field and magnetic induction variations, i.e. $\mathbf{H}_{ec}$ and $\mathbf{B}_{ec}$, respectively.

We apply the transformation $t \rightarrow t' - t$, which performs a temporal reflection and a shift of the time axis, to (47),(48) resulting to the adjoint set of equations

$$\nabla \times \mathbf{E}_{ec}^\dagger = \frac{d\mathbf{B}_{ec}^\dagger}{dt} \tag{49}$$

$$\nabla \times \mathbf{H}_{ec}^\dagger = \mathbf{0}. \tag{50}$$

with the adjoint electric and magnetic fields $\mathbf{E}^\dagger = \mathbf{E}^\dagger(\mathbf{r},t)$ and $\mathbf{H}^\dagger = \mathbf{H}^\dagger(\mathbf{r},t)$, which are linked with the original solution of

Integrating (55) in time, taken into account the previous relation for the boundary integral and rearranging the terms we arrive at the equation

$$\int_0^{t'} dt \int_V \mathbf{E}_{ec}^\dagger \cdot \mathbf{J} dV$$

$$= -\frac{1}{\mu_0} \left[\oint_{\partial V} (\mathbf{A}_{ec} \times \nabla \times \mathbf{A}_s) \cdot \mathbf{e}_n dS - \int_V \mathbf{B}_{ec}^\dagger \cdot \mathbf{B}_s dV \right]_0^{t'}$$

$$+ \frac{1}{\mu_0} \int_0^{t'} dt \oint_{\partial V} \left(A_{ec}^\dagger \nabla \frac{dA_s}{dt} - \frac{dA_s}{dt} \nabla A_{ec}^\dagger \right) \cdot d\mathbf{S}. \tag{56}$$

Making the assumption that the **the system initially is in the zero state** and that **the excitation current starts from zero value** the first term of the right-hand-side vanishes since $\mathbf{A}_s(\mathbf{r},0) = 0$ and $\mathbf{A}_{ec}^\dagger(\mathbf{r},t') = \mathbf{A}_{ec}(-\mathbf{r},0) = 0$. Furthermore, the left-hand-side is equal to the time convolution of the EMF at the pick-up coil with the excitation current $\Delta V(t') * I(t')$, yielding the relation

$$\Delta V(t') * I(t') = \frac{1}{\mu_0} \oint_{\partial V} \left(A_{ec} * \nabla \frac{dA_s}{dt} - \frac{dA_s}{dt} * \nabla A_{ec} \right) \cdot d\mathbf{S} \tag{57}$$

with $(\bullet * \bullet)$ standing for the time convolution integral. Equation (57) provides a very elegant way of calculating the EMF of the receiving coil, in direct analogy with the classical Auld's reciprocity formula [21], [22] for the impedance variation calculations in harmonic problems.

REFERENCES

[1] C. V. Dodd and W. E. Deeds, "Analytical solutions to eddy current probe coil problems," vol. 39, no. 6, pp. 2829–2838, May 1968.

[2] C. V. Dodd, C. C. Cheng, and W. E. Deeds, "Induction coils coaxial with an arbitrary number of cylindrical conductors," vol. 45, no. 2, pp. 638–647, Feb. 1974.

[3] Y. Li, G. Y. Tian, and A. Simm, "Fast analytical modelling for pulsed eddy current evaluation," *NDT & E Int.*, vol. 41, pp. 477–483, 2008.

[4] T. Theodoulidis, H. Wang, and G. Y. Tian, "Extension of a model for eddy current inspection of cracks to pulsed excitations," *NDT & E Int.*, vol. 47, pp. 144–149, 2012.

[5] V. O. de Haan and P. A. de Jong, "Analytical expressions for transient induction voltage in a receiving coil due to a coaxial transmitting coil over a conducting plate," *IEEE Trans. Magn.*, vol. 40, no. 2, pp. 371–378, Mar. 2004.

[6] S. Xie, Z. Chen, T. Takagi, and T. Uchimoto, "Efficient numerical solver for simulation of pulsed eddy-current testing signals," *IEEE Trans. Magn.*, vol. 47, no. 11, pp. 4582–4591, 2011.

[7] ——, "Development of a very fast simulator for pulsed eddy current testing signals of local wall thinning," *NDT & E Int.*, vol. 51, pp. 45–50, 2012.

[8] S. Xie, Z. Chen, H.-E. Chen, X. Wang, T. Takagi, and T. Uchimoto, "Sizing of wall thinning defects using pulsed eddy current testing signals based on a hybrid inverse analysis method," *IEEE Trans. Magn.*, vol. 49, no. 5, pp. 1653–1656, 2013.

[9] J. Bowler and M. Johnson, "Pulsed eddy-current response to a conducting half-space," *IEEE Trans. Magn.*, vol. 33, no. 3, pp. 2258–2264, May 1997.

[10] F. Fu and J. Bowler, "Transient eddy-current driver pickup probe response due to a conductive plate," *IEEE Trans. Magn.*, vol. 42, no. 8, pp. 2029–2037, Aug. 2006.

[11] T. Theodoulidis, "Developments in calculating the transient eddy-current response from a conductive plate," *IEEE Trans. Magn.*, vol. 44, no. 7, pp. 1894–1896, July 2008.

[12] A. Skarlatos and T. Theodoulidis, "A modal approach for the solution of the non-linear induction problem in ferromagnetic media," *IEEE Trans. Magn.*, vol. 55, no. 2, p. 7000211, Feb. 2016.

[13] T. Theodoulidis and A. Skarlatos, "Efficient calculation of transient eddy current response from multilayer cylindrical conductive media," *Phil. Trans. R. Soc. A*, vol. 378, p. 20190588, 2020.

[14] M. Clemens and T. Weiland, "Transient eddy-current calculation with the FI-method," *IEEE Trans. Magn.*, vol. 35, no. 3, pp. 1163–1166, May 1999.

[15] A. Skarlatos, M. Clemens, and T. Weiland, "Start vector generation for implicit Newmark time integration of the wave equation," *IEEE Trans. Magn.*, vol. 42, no. 4, pp. 631–634, Oct. 2006.

[16] J. Dutiné, M. Clemens, S. Schöps, and G. Wimmer, "Explicit time integration of transient eddy current problems," *Int. J. Numer. Modell.*, pp. jnm.2227–n/a, 2017.

[17] A. Skarlatos and T. Theodoulidis, "Study of the non-linear eddy-current response in a ferromagnetic plate: Theoretical analysis for the 2D case," *NDT & E Int.*, vol. 93, no. Supplement C, pp. 150–156, Jan. 2018.

[18] T. P. Theodoulidis and E. E. Kriezis, *Eddy Current Canonical Problems (with applications to nondestructive evaluation)*. Forsyth GA: Tech Science Press, 2006.

[19] T. Theodoulidis and J. Bowler, "Eddy-current interaction of a long coil with a slot in a conductive plate," *IEEE Trans. Magn.*, vol. 41, no. 4, pp. 1238–1247, Apr. 2005.

[20] A. Skarlatos and T. Theodoulidis, "Calculation of the eddy-current flow around a cylindrical through-hole in a finite-thickness plate," *IEEE Trans. Magn.*, vol. 51, no. 9, p. 6201507, Sept. 2015.

[21] B. A. Auld, "Theoretical characterization and comparison of resonant-probe microwave eddy-current testing with conventional low-frequency eddy-current methods," in *Eddy-Current Characterization of Material and Structures*, George Birnbaum and George Free, Eds., American Society for Testing and Materials, Ed., vol. 12, 1981, pp. 332–347.

[22] B. A. Auld, F. Muennemann, and D. K. Winslow, "Eddy current probe response to open and closed surface flaws," *J. Nondestr. Eval.*, vol. 2, no. 1, pp. 1–21, 1981.

[23] W. J. Welch, "Reciprocity theorems for electromagnetic fields whose time dependence is arbitrary," *IRE Trans. Antennas Propagat.*, vol. 8, no. 1, pp. 68–73, Jan. 1960.

[24] ——, "Comments on "Reciprocity theorems for electromagnetic fields whose time dependence is arbitrary"," *IRE Trans. Antennas Propagat.*, vol. 9, no. 1, pp. 114–115, Jan. 1961.

[25] B. Cheo, "A reciprocity theorems for electromagnetic fields with general time dependence," *IRE Trans. Antennas Propagat.*, vol. 13, no. 2, pp. 278–284, Mar. 1965.

[26] A. de Hoop, "Time-domain reciprocity theorems for electromagnetic fields in dispersive media," *Radio Sci.*, vol. 22, no. 7, pp. 1171–1178, 1987.

[27] A. de Hoop, I. E. Lager, and V. Tomassetti, "The pulsed-field multiport antenna system reciprocity relation and its applications — a time-domain approach," *IEEE Trans. Antennas Propag.*, vol. 57, no. 3, pp. 594–605, Mar. 2009.

[28] A. Shlivinski, E. Heyman, and R. Kastner, "Antenna characterization in the time-domain," *IEEE Trans. Antennas Propag.*, vol. 45, no. 7, pp. 1140–1148, July 1997.

[29] A. Shlivinski, "Time-domain coupled response of antennas - reciprocity theorem approach," *IEEE Trans. Antennas Propag.*, vol. 65, no. 4, pp. 1714–1727, Apr. 2017.

[30] T. P. Theodoulidis and J. R. Bowler, "Impedance of an induction coil at the opening of a borehole in a conductor," vol. 103, no. 2, pp. 024 905–1–024 905–9, Jan. 2008.

[31] A. Skarlatos and T. Theodoulidis, "Solution to the eddy-current induction problem in a conducting half-space with a vertical cylindrical borehole," *Proc. R. Soc. London, Ser. A*, vol. 468, no. 2142, pp. 1758–1777, June 2012.

[32] A. Skarlatos, "A mixed spatial-spectral eddy-current formulation for pieces with one symmetry axis," *IEEE Trans. Magn.*, vol. 56, no. 9, pp. 1–11, Sept. 2020.

[33] L. B. Felsen and N. Marcuvitz, *Radiation and Scattering of Waves*. New York: IEEE Press, 1994.